

Particle model for nonlocal heat transport in fusion plasmas

H. Bufferand

Aix-Marseille Université, Laboratoire M2P2-CNRS UMR 7340, 38, rue Frédéric Joliot-Curie, 13451 Marseille, France

G. Ciraolo

Ecole Centrale Marseille, Laboratoire M2P2-CNRS UMR 7340, 38, rue Frédéric Joliot-Curie, 13451 Marseille, France

Ph. Ghendrih

CEA-IRFM, F-13108 Saint-Paul-lez-Durance, France

S. Lepri

Consiglio Nazionale delle Ricerche, Istituto dei Sistemi Complessi via Madonna del piano 10, I-50019 Sesto Fiorentino, Italy

R. Livi

Dipartimento di Fisica e Centro Interdipartimentale per lo Studio delle Dinamiche Complesse, Università di Firenze, via G. Sansone 1, I-50019 Sesto Fiorentino, Italy

(Received 12 June 2012; published 7 February 2013)

We present a simple stochastic, one-dimensional model for heat transfer in weakly collisional media as fusion plasmas. Energies of plasma particles are treated as lattice random variables interacting with a rate inversely proportional to their energy schematizing a screened Coulomb interaction. We consider both the equilibrium (microcanonical) and nonequilibrium case in which the system is in contact with heat baths at different temperatures. The model exhibits a characteristic length of thermalization that can be associated with an interaction mean free path and one observes a transition from ballistic to diffusive regime depending on the average energy of the system. A mean-field expression for heat flux is deduced from system heat transport properties. Finally, it is shown that the nonequilibrium steady state is characterized by long-range correlations.

DOI: [10.1103/PhysRevE.87.023102](https://doi.org/10.1103/PhysRevE.87.023102)

PACS number(s): 52.25.Fi, 05.60.-k, 44.10.+i

I. INTRODUCTION

A key issue of contemporary statistical mechanics is to understand the behavior of systems steadily kept out of equilibrium. In this general framework, confined plasmas represent one of the most relevant playgrounds where a deeper comprehension of transport and relaxation processes would lead to progress in the control of experimental setups. A typical problem is that of heat transfer in the direction parallel to the magnetic field in tokamaks [1,2]. In these devices, the plasma is confined by a strong magnetic field so that the symmetry of transport is split into the plane transverse to the magnetic field where turbulence governs the heat flux and the direction parallel to the magnetic field where turbulent effects are small and collisional transport must be taken into account. Collisions in such plasmas are weak binary Coulomb interactions whose mean free path scales like the fourth power of particle velocity, exceeding by a couple of orders of magnitude the device largest scale in the hot core region. In practice this has little impact on transport issues since temperature remains roughly constant along the magnetic field so that transport effect remains weak in that direction. The issue of parallel transport becomes stringent when a hot plasma region is connected to a wall component. In that case a significant temperature gradient will build up along the field line between the hot region that acts as a heat source and the colder plasma region at the wall that acts as a sink [3]. When collisionality drops, classical Fourier law [4] fails in describing heat transport, leading to an overestimation of the heat flux. Kinetic approaches have been proposed to study transition from strongly collisional to collisionless

regime [5,6]. In that perspective, simplified Fokker Planck simulations have been performed since the early 1980s in order to study and quantify the deviations from the classical Spitzer Harm thermal conductivity [7–9]. An important effort has been made to recast these kinetic effects into a fluid description of heat transport, a point particularly relevant for the development of efficient hydrodynamic tools for fusion plasma. Several nonlocal formulations have been proposed both for magnetically confined and laser created fusion plasmas [10–15]. They consist in generalizing the Fourier's law with a convolution product and an appropriate delocalization kernel that takes the finite length of the system into account, as exemplified by the generalized constitutive equation:

$$J(x) = \int w(x, x') \kappa(x') \nabla T(x') dx', \quad (1)$$

where J is the heat flux, w the delocalization kernel, k the classical Spitzer Harm collisional conductivity, and T the temperature. These kind of formulations have been also generalized to describe radial turbulent transport of heat flux (recent results in Ref. [16]).

We address the problem of weak collisional closure for heat flux in a simplified framework without taking into account the whole complexity of fusion devices. This allows one to investigate the key nonequilibrium effects, such as the lack of local thermalization, in a tractable approach that will shed light into the minimal model required to properly tackle the more complex issues in actual tokamaks.

A considerable insight on the nature of nonequilibrium steady states has been achieved by considering simple stochastic models that describe interaction among “particles” at the mesoscopic level. This class of systems has the invaluable advantage of being pretty straightforward to simulate by Monte Carlo type of methods and, in some cases, to allow for an analytical solution, which is usually unfeasible in the deterministic cases. Actually, many general properties of nonequilibrium states are inferred by such simplified models, thus opening the way to general concepts and approaches [17,18]. For heat conduction problems [19–21], the simplest level of modeling amounts to considering local energies as random variables on a lattice [22]. In this context, a model that can be explicitly solved is the Kipnis-Marchioro-Presutti (KMP) lattice model, in which stochastic collisions mix the energy of neighboring particles, conserving the total energy [23]. This model is proven to satisfy Fourier’s law when put in contact with two external reservoirs yielding a linear temperature profile. Energy-conserving stochastic noise has been also used in lattice model systems, as natural generalizations of KMP and of the simple exclusion process [24]. In the same perspective, lattices of coupled oscillators subject to energy- and momentum-conserving noise have been also discussed to describe anomalous heat conduction problems and the associated steady-state correlations properties [25,26]. In this paper, we introduce a simple one-dimensional (1D) stochastic model that contains the minimum ingredients to study the properties of the transition from local to nonlocal transport. The dynamics inspired by the above-mentioned KMP model [23] is supplemented by interaction rules introduced to describe the salient features of Coulomb interaction and leading to an energy-dependent thermalization mean free path.

In the same spirit we aim at bringing new understanding of transport properties of plasma starting from such simplified models. Indeed in the fusion plasma community there is an urgent need for understanding and predicting the heat flux impacting the materials, a crucial point for the device performance. On the other hand, data interpretation from the large kinetic codes usually employed in the theoretical analysis is not straightforward due to the complexity of the magnetic topology and the many physical mechanisms at play. Simplified models would provide a better insight and guidance for that interpretation. However, one must then aim at removing any free parameter that cannot be fixed by available experimental evidence. Determining the appropriate and accurate transport properties then relies on dedicated investigation of the underlying mechanisms [Eq. (1)], as addressed in the present paper.

The paper is organized as follows. In Sec. II the stochastic model is presented, and the interaction rule between particles as well as the probability of the energy exchange are introduced. In Sec. III we study the equilibrium properties of the system as a function of its average energy. In particular, the thermal diffusivity is computed using both the Green Kubo formula and nonequilibrium simulations. Then, in Secs. IV and V, we analyze the transport properties of the stochastic model using the telegraph equation. This mean-field description is obtained using a generalized Fourier’s law with a delocalization kernel exponentially decaying in time and space. Finally, spatial correlations in the nonequilibrium

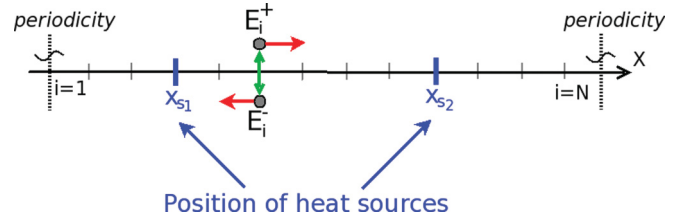


FIG. 1. (Color online) Sketch of the 1D particle model. The dynamic step is represented with red (dark gray) horizontal arrows; the interaction step is represented with green (light gray) vertical arrows.

steady state are investigated in Sec. VI and conclusions and discussions are presented in Sec. VII.

II. DESCRIPTION OF THE MODEL

We aim at characterizing plasma heat transport with a probabilistic model. This model is sketched in Fig. 1. At each lattice site $i = 1, \dots, N$ we have a pair of particles of energies E_i^+ and E_i^- : the plus and the minus sign indicates particles moving in opposite directions with constant velocity. Their discrete-time dynamics consists of two steps. At each time t , we first perform a free convection of energy:

$$E_i^\pm(t) \longrightarrow E_{i\pm 1}^\pm(t'). \quad (2)$$

We assume periodic boundary conditions assumed as for a ring geometry. Taking inspiration from the KMP model, we consider that the energy exchange mechanism between particles occurs at each lattice site i at any time t and amounts to a random redistribution of the total energy of the particles. In formulas

$$\begin{aligned} E_i^+(t+1) &= r[E_i^+(t') + E_i^-(t')] = 2rE_i(t'), \\ E_i^-(t+1) &= (1-r)[E_i^+(t') + E_i^-(t')] = 2(1-r)E_i(t'), \end{aligned} \quad (3)$$

where we have defined the energy on the site i as $E_i(t) = [E_i^+(t) + E_i^-(t)]/2$ and with r a random number uniformly distributed in $[0, 1]$.

In order to include an important ingredient coming from the physics of the interactions among plasma particles, we mimic an effective Coulomb-like cross section by assuming that the energy exchange may occur with a rate \mathcal{P} inversely proportional to the square of the energy of the interacting particles. Specifically,

$$\mathcal{P} = \frac{C}{1 + (E_i/E_{\text{int}})^2}, \quad (4)$$

where E_{int} is an energy scale, $0 < E_i < +\infty$, and C is a suitable constant. For $E_i \ll E_{\text{int}}$, the interaction probability is energy independent meaning that low-energy particles are strongly interacting. In this asymptotic limit, rule (4) is expected to yield a standard diffusion mechanism. On the other hand, for $E_i \gg E_{\text{int}}$ the collision rate vanishes and thus particles travel almost ballistically.

In tokamaks, plasma particles interact with hot and cold localized sources (e.g., fast particle heated region, hot-cold turbulent structures, etc.) that are schematized as external reservoirs. We can introduce two heat sources located at the lattice sites i_h and i_c (typically $i_h \sim N/4$ and $i_c \sim 3N/4$)

and with inverse temperatures β_h, β_c , respectively. To keep the interaction rule as simple as possible and in analogy with other models of heat baths [20], we assume a strong coupling with the sources: at each time step, energies E_i^\pm , at the source sites $i = i_h, i_c$ are assigned new random values drawn from the Maxwell-Boltzmann distributions $\beta_h \exp(-\beta_h \epsilon)$ and $\beta_c \exp(-\beta_c \epsilon)$, respectively.

In the simulation hereby discussed, the update is synchronous on all lattice sites; one could make it sequential by updating randomly chosen sites from a uniform distribution, but we do not expect significant modifications with respect to the synchronous rule.

A related mean-field model has been discussed in Ref. [27].

III. STUDY OF THE EQUILIBRIUM PROPERTIES: CHARACTERISTIC THERMALIZATION SCALE

A. Relaxation to equilibrium

In order to study the equilibrium, we consider a domain without sources and let the system evolve starting from an arbitrary random state. Let us denote by $f(E, t)$ the distribution function of energies of all particles at time t . As an example, we consider the case that the energies of the particles are initialized with $f(E, 0)$ being a step distribution function centered on the average energy E_0 (see the curve labeled $t = 0$ in Fig. 2). As expected, after a certain number of time steps, $f(E, t)$ approaches a Maxwell-Boltzmann distribution $f_0(E) = \beta \exp(-\beta E)$ where $\beta = 1/T = 1/E_0$; see Fig. 2(a). To monitor this convergence to equilibrium we considered the distance $d(t) = \langle \|f(E, t) - f_0(E)\| \rangle$. The $\| \cdot \|$ denotes \mathcal{L}^1 norm while $\langle \cdot \rangle$ means an average over several trajectories. At long enough times, this distance decays exponentially to zero $d = F \exp(-t/\tau_r)$; see Fig. 2(b). Actually, a closer inspection of the data suggests that the equilibration process occurs in two stages, compatible with a double exponential fit. We can argue that the first time scale is associated to some transient equilibration that may depend on the chosen initial conditions. What actually governs the asymptotic behavior of the relaxation to equilibrium is the final stage characterized by

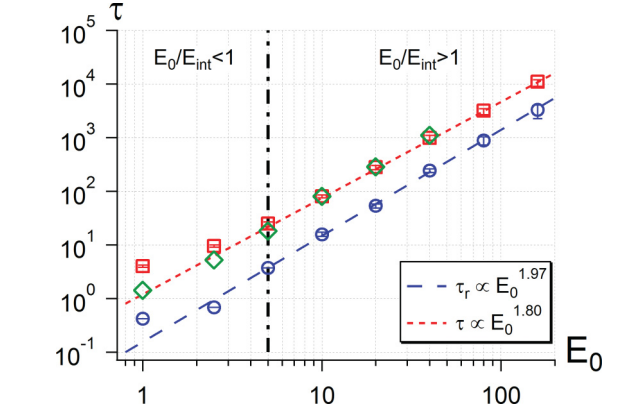
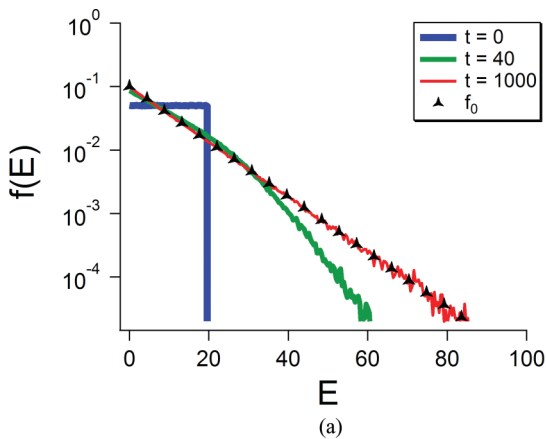


FIG. 3. (Color online) Characteristic times of the interaction as a function of system average temperature E_0 . Blue dots: relaxation time to equilibrium; see Sec. III A. Red squares: fitting value of τ in Eq. (14). Green diamonds: cutting time $\tau_c = 1/\omega_c$. Lines: power law fit.

a time scale that we denote τ_r . Numerical evidence suggests that the latter time scale is proportional to the square of the average energy, $\tau_r \propto E_0^2$ (see the lower line in Fig. 3). This is a consequence of the choice of the interaction rate \mathcal{P} in Eq. (4). More precisely, the relaxation time τ_r can be seen as the number of events required for probability of having interacted to be of order 1, that is for independent events $\tau_r \mathcal{P} = 1$.

B. Fluctuations around equilibrium

In the spirit of linear-response theory, properties of the fluctuations of equilibrium currents yield information on transport coefficients. In the present context we are interested in the correlation function of the heat current J , $c_J(\tau) = \langle J(t)J(t - \tau) \rangle$, whose time integral is related to the thermal diffusivity by the Green-Kubo formula [28]

$$D = \frac{1}{k_B T^2 N} \int_0^\infty c_J(\tau) d\tau, \quad (5)$$

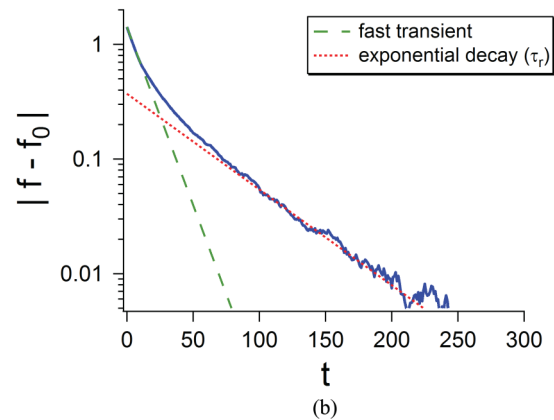


FIG. 2. (Color online) Relaxation to equilibrium for $N = 1000$ particle sites, $E_0 = 10$, and $E_{\text{int}} = 5$. (a) Initial (thick blue), transient (green), and equilibrium (thin red) distribution of energy; symbols: equilibrium exponential distribution f_0 . (b) Distance to equilibrium distribution versus time. Full blue: simulation results; dotted red: fit with exponential decay with decay time τ_r ; dashed green: fast transient relaxation of initial conditions.

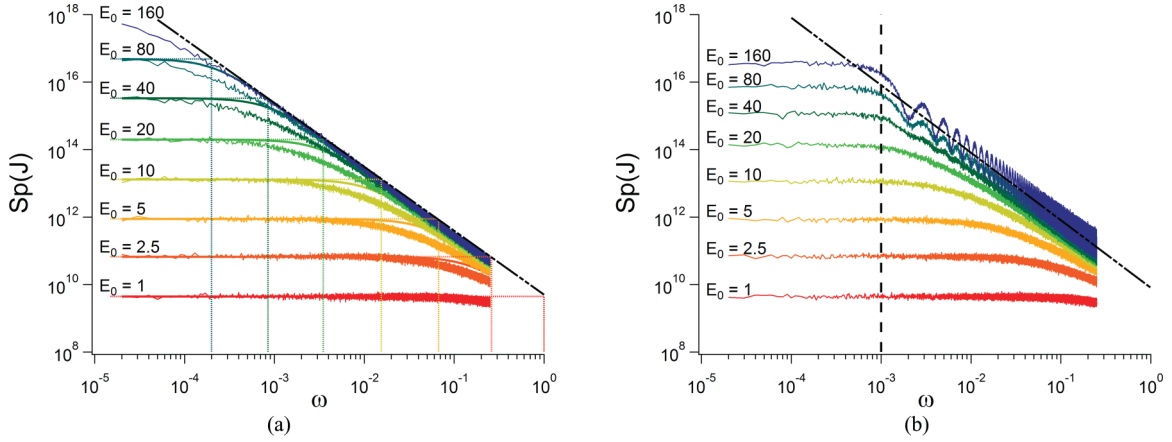


FIG. 4. (Color online) Power spectrum of total heat flux for different average energies E_0 . Simulation parameters: $N = 1000$ and $E_{\text{int}} = 5$. The black line represents the ω^{-2} asymptotic behavior. (a) Results without sources and fits with Lorentzian. The vertical lines correspond to the respective cutting frequency ω_c . (b) Results with sources. The vertical dashed line indicates the characteristic frequency associated with system size ω_{system} . Units on the vertical axis are arbitrary.

where T is the equilibrium temperature of the system defined above and N the number of sites, defining the length of the system. We ignore here the difference between diffusivity and conductivity since they only differ by a proportionality constant. More generally, the time behavior of c_J yields information on relaxation processes and thus on nonstationary energy transport. By Wiener-Khintchin theorem, this description is equivalent to considering the power spectrum $Sp[J](\omega) = \mathcal{F}[c_J(\tau)]$ where \mathcal{F} denotes the Fourier transform.

In our model, the heat flux at site i is defined as $j_i(t) = E_{i-1}^+(t) - E_i^-(t)$ as can be found by writing the lattice continuity equation $E_i(t+1) - E_i(t) = -j_{i+1} + j_i$. The total heat flux traveling in the system is the sum of all the local contributions $J(t) = \sum_i j_i(t)$.

The application of Green-Kubo formula for open, finite systems is still a matter of debate [29], so it is relevant to perform a comparison between different statistical ensembles. In a first series of experiments, we considered the microcanonical system with the sources turned off. In Fig. 4(a) we plot the power spectra of J for different values of the system energy E_0 . The data are fitted with a Lorentzian shape, i.e., $Sp[J](\omega) \approx C/(\omega^2 + \tau_c^{-2})$, assuming that the time correlation function c_J decays exponentially with a single¹ characteristic time scale τ_c . From the data we found that $\tau_c \sim E_0^2$, see the lower line in Fig. 3, namely the same dependence of the thermalization time τ_r .

The time τ_c defines a characteristic length λ_c which represents a particle mean free path. Indeed, if a particle moves on a length smaller than λ_c (or on a time smaller than τ_c), the interaction probability is very small and the transport of energy can be considered as ballistic. On the contrary, on scales larger than λ_c , it is likely that a particle undergoes

several interaction events hence reducing its correlation with its initial conditions. The particle thermalizes and the energy transport can be thereby described as a standard diffusion process.

This observation is useful to interpret the data for the canonical case in which the system interacts with two sources both having the same temperatures $\beta_h = \beta_c$ corresponding to an average system energy equal to the value E_0 employed in the microcanonical setting. The heat flux power spectra for different values of E_0 are reported in Fig. 4(b).

At small enough energies $\lambda_c \ll N$ microcanonical and canonical spectra are almost the same (compare the lower lying curves in Fig. 4). Conversely, for larger E_0 ($\lambda_c \sim N$) differences are significant. In particular, in the presence of sources the spectra display oscillations. This is a consequence of the presence of localized thermal sources in the lattice. More precisely, the particle transit time τ_s between the sources corresponds to the characteristic time of the oscillations of the spectra. Despite this oscillating behavior, one observes at any value of E_0 a flat profile of the spectra for small frequencies, $\omega < 1/\tau_s$. This is due to the fact that particles lose memory when interacting with the sources and no correlation can be expected for times larger than τ_{sources} .

Another difference between the microcanonical and the canonical cases is shown in Fig. 5 where the thermal diffusivity as a function of the average energy of the system is shown. One can conclude that the Green-Kubo relation (5) evaluated in these two ensembles yields the same result only for small enough energies. For a high value of E_0 , a quasiballistic regime where D grows proportionally to E_0^2 is observed for the microcanonical data, while the canonical data exhibit a saturation of the ballistic regime and D levels off at half of the system length $N/2$. This upper bound is reached because any particle must at least interact with the sources. These results can be explained from the following considerations on the Green-Kubo formula:

$$D = \frac{1}{NT^2} \int_0^\infty c_J(\tau) d\tau \approx \frac{1}{NT^2} \langle J^2 \rangle \tau_{\text{cor}},$$

¹Admittedly, the Lorentzian fit is not very accurate for $\omega\tau_c \sim 1$. A possible improvement would be to consider a two-parameter fitting with two characteristic time scales, somehow akin with the two relaxation stage illustrated in Fig. 2. For simplicity, we ignored this refinement henceforth.

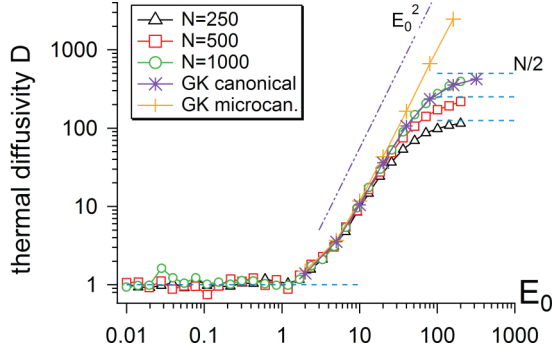


FIG. 5. (Color online) Comparison of heat diffusivities computed by nonequilibrium simulations for three different lattice sizes (circles, squares, and triangles) and with Kubo-Green formula ($N = 1000$, $E_{\text{int}} = 5$); stars and crosses correspond to the data with and without sources, respectively. The horizontal lines mark the two asymptotic values $D \approx 1$ and $D \approx N/2$; for comparison we draw a line corresponding to $D \sim E_0^2$ (dash-dotted).

where τ_{cor} is defined as the characteristic correlation time. From equilibrium distribution of energy, the local heat flux j_i can be described by a normal law centered on zero and with a standard deviation of $\sqrt{2T}$ and, consequently, the total heat flux $\langle J^2 \rangle = \langle \sum_{i=1}^N j_i \rangle = 2NT^2$. Concerning the correlation time, one can distinguish between three cases. For small enough temperatures such that the particle mean free path is shorter than the distance between the sources, the correlation time is inversely proportional to the probability rate of interaction $\tau_{\text{cor}} = 1/\mathcal{P}$. For high energies E_0 , the mean free path becomes larger than the distance between sources and the correlation time is then the transit time $\tau_s = N/2$. The threshold between collisional and ballistic regime is reached for $E_0 > \sqrt{N/2}E_{\text{int}} = E_{\text{ball}}$. One finally obtains

$$D \approx \begin{cases} 1 & \text{if } E_0 \ll E_{\text{int}}, \\ \left(\frac{E_0}{E_{\text{int}}}\right)^2 & \text{if } E_{\text{int}} < E_0 < E_{\text{ball}}, \\ \frac{N}{2} & \text{if } E_{\text{ball}} < E_0. \end{cases} \quad (6)$$

For comparison, in Fig. 5 we report also the values of D computed by nonequilibrium simulations. Those are obtained by computing the average heat current divided by the applied gradient $2(\beta_c^{-1} - \beta_h^{-1})/N$. The temperature difference is fixed to 20% of the average, to ensure that the gradient is small for the considered sizes. The current can be evaluated by averaging either the energies exchanged with the sources or the above defined current, J . Equality of such two quantities (within statistical fluctuations) is checked to ensure that the steady state is attained on the time scale of the numerical simulations (typically 10^5 time steps). It is noteworthy that the canonical Green-Kubo data accounts very accurately for the nonequilibrium measurements of the finite system.

IV. GENERALIZED FOURIER LAW

The first step to analyze the transport properties of the stochastic model is to determine whether the energy flux can be expressed using the linear-response approach. At a macroscopic level, one uses the most general linear relation between the energy current J and the local temperature

gradient. Precisely, one can express the heat flux with a generalized Fourier law where J takes the form of the spatiotemporal convolution of the temperature gradient with a memory kernel K [30],

$$J(x,t) = - \int_{-\infty}^{\infty} dx' \int_{-\infty}^t dt' K(x-x', t-t') \frac{\partial T}{\partial x}(x', t'). \quad (7)$$

The temporal evolution of the temperature field is given (up to some dimensional constant) by the heat equation:

$$\frac{\partial T}{\partial t}(x,t) = - \frac{\partial J}{\partial x}(x,t). \quad (8)$$

Making use of the Laplace-Fourier transform

$$\tilde{Y}(k, \omega) = \int_{-\infty}^{\infty} dx \int_0^{\infty} dt Y(x,t) e^{i(kx - \omega t)},$$

Eqs. (7) and (8) yield the relation

$$\tilde{T}(k, \omega) = \frac{\mathcal{F}[T(x,0)](k)}{i\omega - k^2 \tilde{K}(k, \omega)}, \quad (9)$$

where $\mathcal{F}[T(x,0)]$ is the Fourier transform of the initial data.

The simplest phenomenological form of the kernel is the one in which memory decays exponentially in both time and space,

$$K(x,t) = \frac{D}{2\lambda\tau} \exp\left(-\frac{t}{\tau}\right) \exp\left(-\frac{|x|}{\lambda}\right), \quad (10)$$

where τ and λ are the characteristic time and space scales above which the heat transfer can be described by a diffusion process. In the definition we choose the coefficients in such a way that the usual Fourier law $J = -D \frac{\partial T}{\partial x}$ is recovered for a constant and time-independent temperature gradient. The Laplace-Fourier transform of K is thus given by

$$\tilde{K}(k, \omega) = \frac{D}{(1 - i\tau\omega)(1 + \lambda^2 k^2)}. \quad (11)$$

This means that $\tilde{T}(k, \omega)$ may have poles at complex frequencies and thus that relaxation may occur in the form of damped heat waves [30]. In order to obtain some insight on what to expect from our model, let us for the moment drop the terms in λ . The Laplace-Fourier transform of the heat equation then reduces to

$$\tilde{T}(k, \omega) = \frac{\mathcal{F}[T(x,0)](k)(-i\omega + 1/\tau)}{-\omega^2 - i\omega/\tau + Ak^2}, \quad (12)$$

which [assuming $\partial_t T(x,t) = 0$ for $t = 0$] is also the Laplace-Fourier transform of the telegraph equation [30]:

$$\frac{\partial^2 T}{\partial t^2} + \frac{1}{\tau} \frac{\partial T}{\partial t} = A \frac{\partial^2 T}{\partial x^2}. \quad (13)$$

For $\tau \ll 1$, that is to say a short mean free path, the telegraph equation becomes the equation of diffusion with a diffusion coefficient $A\tau$. For $\tau \gg 1$, the first derivative vanishes and one finds the wave-propagation equation with a wave velocity $v = \sqrt{A}$.

V. NUMERICAL EVIDENCES OF MEMORY EFFECTS

In this section, we perform numerical simulations with the stochastic model to investigate if its behavior can be described by this effective formulation.

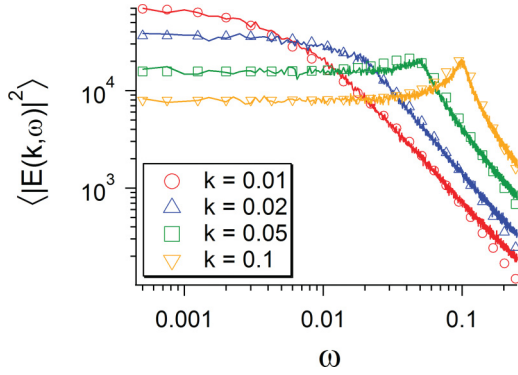


FIG. 6. (Color online) Dynamical structure factor for $E_0 = 5$. Full lines represent simulation results. One notices the resonance for high values of k denoting a ballistic transport at small scales that differs from the diffusive transport at large scales (no resonance for low value of k). The low-frequency part of the data have been fitted (symbols) with the function $B/[(\omega^2 - \omega_0^2)^2 + (\omega/\tau)^2]$ derived by Eq. (14) under the approximation $\omega \ll 1/\tau$ where the numerator simplifies to a constant.

A. Equilibrium fluctuations

In this part, we study the spatiotemporal evolution of the fluctuations around equilibrium. To compare with the above hydrodynamic approach, we compute numerically the dynamical structure factor $\langle |\tilde{E}(k, \omega)|^2 \rangle$, where $\tilde{E}(k, \omega)$ is the spatiotemporal Fourier transform of the energy field $E_i(t)$. As usual, $\langle \cdot \rangle$ denotes the average over several realizations. One tries to fit the results obtained numerically with the formula found analytically for the time and space exponential memory kernel. According to Eqs. (9) and (11), one obtains

$$\langle |\tilde{E}(k, \omega)|^2 \rangle = \frac{T_0^2(\omega^2 + 1/\tau^2)}{(\omega^2 - \omega_0^2)^2 + (\omega/\tau)^2}, \quad (14)$$

with

$$\omega_0^2 = \frac{D}{\tau} \frac{k^2}{1 + \lambda^2 k^2}. \quad (15)$$

To derive Eq. (14) from Eq. (9), we let

$$\langle |\tilde{E}(k, \omega)|^2 \rangle = \langle |\tilde{T}(k, \omega)|^2 \rangle$$

and assume that the average over the initial random conditions of $\mathcal{F}[T(x, 0)]$ yields a constant denoted by T_0 .

The numerical results and fits are plotted in Fig. 6 in the case $E_0 = E_{\text{int}} = 5$. For high values of k ($k = 0.1$), i.e., at small scales, we observe a peak at finite frequency that indicates some kind of oscillating response, that is the propagation of damped temperature waves. On the contrary, at large scales ($k = 0.01$), the peak disappears and the spectrum shows a monotonic decay that signals the onset of a diffusive behavior. We have also observed that for small (large) values of E_0 , i.e., at low (high) temperature, the behavior is diffusive (ballistic) for all values of k .

Moreover, we find that ω_0 is approximately proportional to k , i.e., typically we are dealing with regimes where $\lambda k \ll 1$.

Where τ is concerned, one finds that it scales as $\tau \sim E_0^2$, which is consistent with the data shown in Fig. 3.

B. Evolution of perturbations

The dynamics of disturbances is a typical nonstationary heat conduction problem [31,32]. From Eq. (12) it is expected that their propagation would display a transition from a diffusive to a wavelike propagation behavior upon increasing the energy. Numerical studies have been performed by “thermalizing” the lattice at energy E_0 according to a Maxwell-Boltzmann distribution and then heating a small domain of the lattice at the energy $1.5E_0$. Figure 7 shows this finite amplitude perturbation propagates in space and time for different values of E_0 .

It can be observed that for small values of E_0 the perturbation diffuses, whereas for $E_0/E_{\text{int}} \gg 1$ one observes the ballistic propagation of two temperature fronts, in qualitative agreement with the telegraph equation (13).

C. Temperature profiles at steady state

In Fig. 8 we plotted three temperature profiles at steady state for different values of the initial average temperature of the system E_0 . For each case, the temperatures of the source are chosen as $E_{\text{hot}}/E_0 = 105\%$ and $E_{\text{cold}}/E_0 = 95\%$. One plots the average temperature E_i as well as the forward-going and backward-going particle temperature (E_i^\pm). One notices that for low values of temperature, one has $E_i \approx E_i^+ \approx E_i^-$ and one recovers a quasilinear profile interpolating between the two source temperatures that is similar to the temperature profile that could be found considering the Fourier law $J = -\kappa \nabla T$. On the contrary, when the temperature is higher, one observes a departure between E_i^+ and E_i^- that is a consequence of the weakness of the interaction for such temperatures. This difference between E_i , E_i^+ , and E_i^- can be seen as the failure of local thermal balance. In this case, the heat transport between the sources is obviously ballistic. When one considers the profile of the average temperature, one notices a quasilinear profile in the region between the sources. However, one observes steep temperature gradients close to the sources. This suggests the existence of a boundary layer around source position.

A possible explanation can be drawn by solving Eq. (8) with the kernel of Eq. (10):

$$J(x) = -\frac{D}{2\lambda} \int_{-\infty}^{\infty} dx' \exp\left(-\frac{|x-x'|}{\lambda}\right) \frac{\partial T}{\partial x}(x'). \quad (16)$$

This expression is quite similar to the one proposed by Luciani [10] to describe heat flux for steep temperature gradients in plasma. The profiles obtained fit quite well with the steady-state solution of the stochastic model (see Fig. 8). Notice that the solution correctly reproduces the temperature drops at the sources, that could not be obtained by the standard Fourier law. More precisely, the Fourier transform of the heat equation gives according to Eq. (11)

$$\frac{Dk^2}{1 + \lambda^2 k^2} \tilde{T} = \tilde{S}, \quad (17)$$

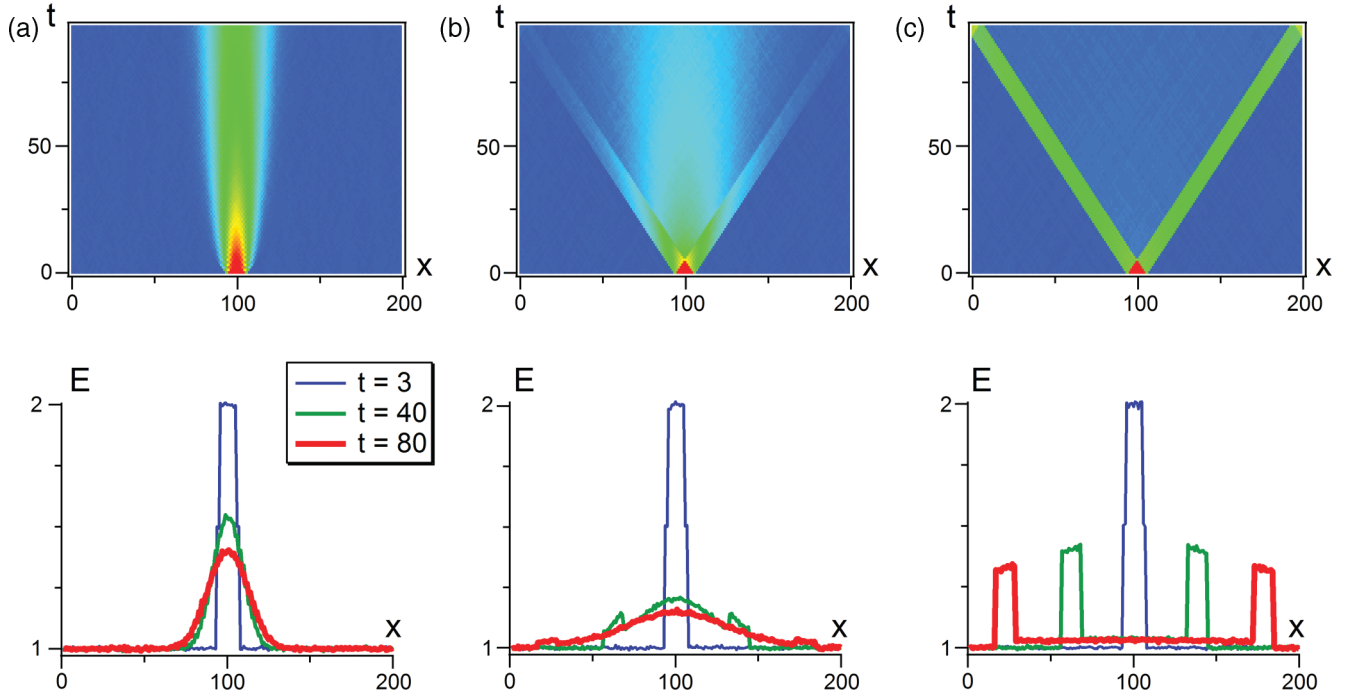


FIG. 7. (Color online) Propagation of a perturbation for different temperatures. (a) Low temperature $E_0/E_{\text{int}} = 0.2$ (diffusive transport). (b) Intermediate temperature $E_0/E_{\text{int}} = 1$. (c) High temperature $E_0/E_{\text{int}} = 4$ (ballistic transport).

where \tilde{S} denotes the Fourier transform of the sources. One notices that this equation can be rewritten as

$$T(x) = T(0) + \frac{\partial T}{\partial x}(0) x + \frac{1}{D} \int_0^x dx' \int_0^{x'} dx'' S(x'') + \frac{\lambda^2}{D} S(x), \quad (18)$$

where $S(x) = S_0[\delta(x - x_h) - \delta(x - x_c)]$ in the case we consider here. The first contribution describes solution of the standard diffusion law. It is the dominant term if $\lambda^2 \ll D$. The second term that becomes dominant if λ is important produces

nonlocal effects and causes the strong gradients localized near sources.

VI. SPATIAL CORRELATIONS IN THE NONEQUILIBRIUM STEADY STATE

In this section, we consider the steady nonequilibrium state with heat sources at different temperatures.

Analogous to what was found in other stochastic and deterministic models [24,26,33], we expect the onset of a nonzero heat flux to be characterized by long-range spatial correlations. In the KMP model, correlations are given by the expression (see [17])

$$C_{ij}^x = \begin{cases} \frac{(T_1 - T_0)^2}{N+1} \frac{i}{N} \left(1 - \frac{j}{N}\right) & \text{if } 0 \leq i < j \leq N, \\ \langle E_i \rangle^2 + 2 \frac{(T_1 - T_0)^2}{N+1} \frac{i}{N} \left(1 - \frac{i}{N}\right) + \frac{(T_1 - T_0)^2}{N(N+1)} & \text{if } 0 \leq i = j \leq N, \end{cases} \quad (19)$$

where the spatial autocorrelation function C_{ij}^x is defined as

$$C_{ij}^x = \langle E_i E_j \rangle - \langle E_i \rangle \langle E_j \rangle \quad (20)$$

and $\langle E_i \rangle$ denotes the value of the mean energy at site i :

$$\langle E_i \rangle = T_0 + (T_1 - T_0) \frac{i}{N}. \quad (21)$$

We have computed numerically C_{ij}^x for our model. For low values of E_0 (diffusive regime) data agrees with theoretical

predictions (that are essentially equivalent in the KMP model), while for large values of E_0 (ballistic regime) no spatial correlation is present (see Fig. 9).

VII. CONCLUSIONS AND DISCUSSIONS

We have presented a 1D stochastic model for studying the main features of heat transport in weakly collisional media. Taking inspiration from the KMP model for collisional heat transfer, we consider an ensemble of N particles moving with

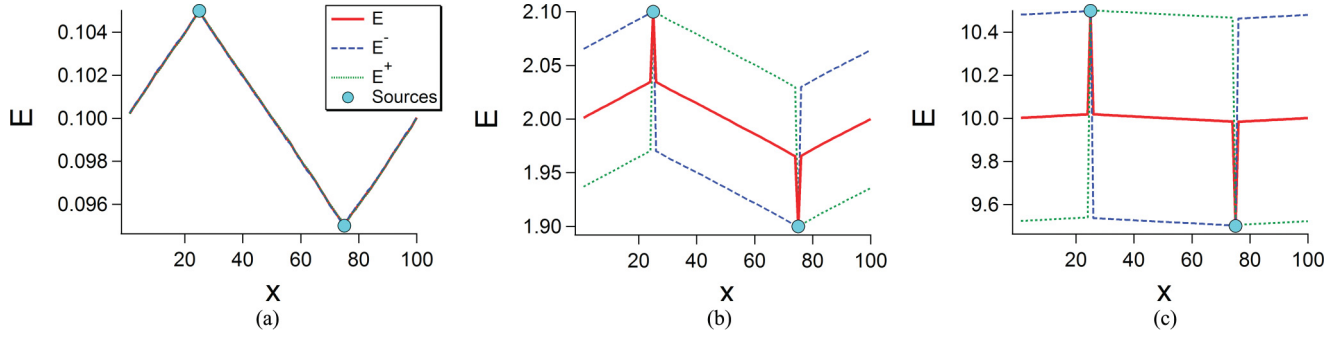


FIG. 8. (Color online) Temperature profiles at steady states with sources for different values of E_0 [(a) $E_0 = 0.1$; (b) $E_0 = 2$; (c) $E_0 = 10$]. For all cases, $E_{\text{int}} = 0.5$.

constant velocity on a ring geometry and with a probability of interaction depending on their energy. The interaction rule is the crucial ingredient that makes this model relevant for plasma physics. Depending on the energy injected in the system, the model is able to describe collisional transport (low-energy case) and the ballistic one (high-energy case), as well as the intermediate cases.

A series of numerical experiments is carried out in order to study equilibrium properties, temporal and spatial memory effects, and the validity of a mean-field description for the observed results. First we have verified that the system relaxes to the Maxwell-Boltzmann distribution of energy with a decay time that has the desired dependence with system temperature. Then interesting results are obtained on thermal diffusivity considering fluctuations around equilibrium. We have estimated thermal diffusivity using the Green Kubo formula, both using microcanonical and canonical simulations. A comparison of the results shows that these estimations coincide for the low-energy case (collisional transport) while increasing the mean energy E_0 of the system and, going toward the ballistic case, the microcanonical diffusivity diverges as E_0^2 while the canonical diffusivity saturates to a value proportional to the distance between the two sources. Nonequilibrium simulations are performed for studying this noncollisional case. One remarks that the canonical Green Kubo data accounts

very accurately for the nonequilibrium measurements of the finite system.

In the second part of the paper we investigate spatiotemporal memory effects of heat transport simulations and how they vary depending on the average energy of the system. A generalized formulation of the Fourier law is introduced and a delocalization kernel exponentially decaying in time and space is assumed. In this case we show that the heat equation corresponds to the telegraph equation. It is noteworthy that this macroscopic description accounts very well for the numerical results obtained from the stochastic microscopic dynamics. The spectral analysis of energy fluctuations around equilibrium shows that for small scales and intermediate values of the average energy, damped temperature waves propagate into the system as expected from the telegraph equation. More generally, we have verified that the telegraph equation properly encompasses the transition from diffusive to ballistic transport according to system collisionality.

Besides, the stochastic model also shows spatial memory effects when it is brought out of equilibrium. This analysis is done by studying steady-state energy profiles when localized heat sources are added in the system. The standard linear temperature profile is recovered for low-temperature cases, when the effect of the probability of interaction vanishes and when the system response is properly described by standard

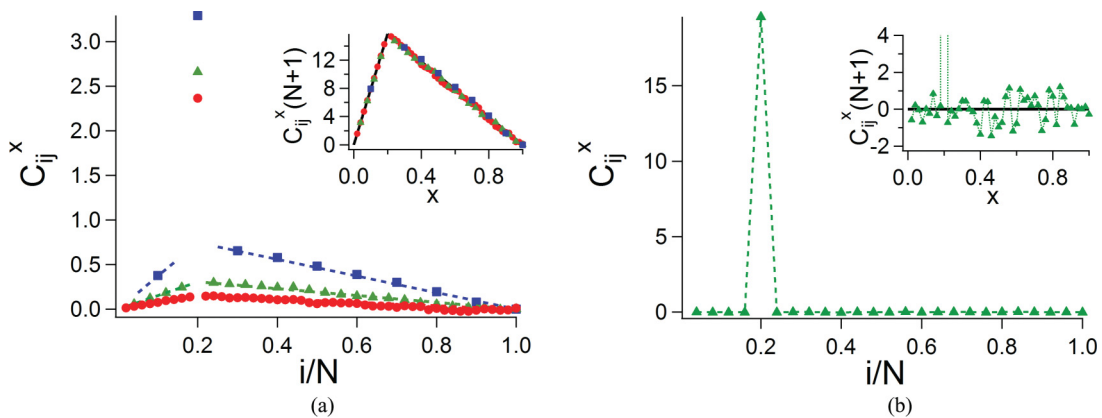


FIG. 9. (Color online) Spatial correlation function close to the cold source for different values of interaction temperature [(a) $E_{\text{int}} = 0.001$; (b) $E_{\text{int}} = 1000$]. Results show spatial correlations at low temperature (left) in good agreement with the analytical model developed in Ref. [17] plotted with lines for different system sizes N [$N = 25$ (blue squares), $N = 50$ (green triangles), and $N = 100$ (red circles)]. At high temperature (right), the spatial correlations disappear. In these simulations, one has $T_1 = 10$ and $T_0 = 0.1$.

Fourier law. On the opposite, when the system temperature is high enough, a boundary layer develops around the sources with steep temperature gradients, as observed experimentally in tokamak edge plasma. These kind of profiles are well described by the generalized Fourier law that we have assumed.

Finally, we point out that the simulation results on heat transport and system response obtained from this first-principle stochastic model are very well described by the nonlocal mean-field formulation we propose, not only in the collisional limit but also when collisionality is very small and local equilibrium breaks.

Based on the results presented here, we are implementing the nonlocal heat flux expression in the transport code SOLEDGE2D [34]. This code simulates the plasma in realistic tokamak geometries and aims at giving quantitative predictions of the heat flux on plasma facing components. A key issue is the thickness of the device boundary layer that is determined by a balance between transverse and parallel transport. As a consequence, well established models that account for the parallel transport are crucial in reducing the uncertainty margin of these key parameters that directly impact the design of the fusion devices. Preliminary results obtained with the nonlocal

form developed here demonstrate that in the high-temperature regimes (low collisional plasmas) the heat flux behavior in the presence of strong temperature gradients is properly described. In particular, the saturation of the heat flux diffusivity, as observed in Fig. 5, appears to be consistent with experimental evidence. Alternative means to describe the parallel transport properties, such as the temperature decoupling in Fig. 8, are also contemplated. The insight given by models that are focused on key basic transport features, as the present work, thus proves most valuable in motivating and directing the effort towards improved descriptions of the transport properties of fusion plasmas.

ACKNOWLEDGMENTS

This work supported by the ANR project ESPOIR and by the European Communities under the contract of Association between EURATOM and CEA was carried out within the framework of the European Fusion Development Agreement. S. Lepri and R. Livi acknowledge financial support from the ENEA-EURATOM Association (Contract No. FU07-CT-2007-00053).

-
- [1] T. C. Hender *et al.*, *Nucl. Fusion* **47**, S128 (2007).
 - [2] W. Fundamenski, *Plasma Phys. Controlled Fusion* **47**, R163 (2005).
 - [3] P. C. Stangeby, *The Plasma Boundary of Magnetic Fusion Devices* (IOP, New York, 2000).
 - [4] L. Spitzer and R. Härm, *Phys. Rev.* **89**, 977 (1953).
 - [5] J. W. Bond and M. P. Gough, *J. Phys. D: Appl. Phys.* **14**, 1153 (1981).
 - [6] M. H. Shirazian and L. C. Steinhauer, *Phys. Fluids* **24**, 843 (1981).
 - [7] A. R. Bell, R. G. Evans, and D. J. Nicholas, *Phys. Rev. Lett.* **46**, 243 (1981).
 - [8] J. P. Matte and J. Virmont, *Phys. Rev. Lett.* **49**, 1936 (1982).
 - [9] J. R. Albritton, *Phys. Rev. Lett.* **50**, 2078 (1983).
 - [10] J. F. Luciani, P. Mora, and J. Virmont, *Phys. Rev. Lett.* **51**, 1664 (1983).
 - [11] J. R. Albritton, E. A. Williams, I. B. Bernstein, and K. P. Swartz, *Phys. Rev. Lett.* **57**, 1887 (1986).
 - [12] S. Krasheninnikov, *Phys. Fluids B* **5**, 74 (1993).
 - [13] V. Y. Bychenkov, W. Rozmus, V. T. Tikhonchuk, and A. V. Brantov, *Phys. Rev. Lett.* **75**, 4405 (1995).
 - [14] G. Schurtz, P. D. Nicolai, and M. Busquet, *Phys. Plasmas* **7**, 4238 (2000).
 - [15] P. D. Nicolai, J.-L. A. Feugeas, and G. Schurtz, *Phys. Plasmas* **13**, 032701 (2006).
 - [16] G. Dif-Pradalier, P. H. Diamond, V. Grandgirard, Y. Sarazin, J. Abiteboul, X. Garbet, P. Ghendrih, A. Strugarek, S. Ku, and C. S. Chang, *Phys. Rev. E* **82**, 025401 (2010).
 - [17] L. Bertini, A. D. Sole, D. Gabrielli, G. Jona-Lasinio, and C. Landim, *J. Stat. Mech.* (2007) P07014.
 - [18] T. Bodineau and B. Derrida, *Comptes Rendus Physique* **8**, 540 (2007).
 - [19] F. Bonetto, J. L. Lebowitz, and L. Rey-Bellet, in *Mathematical Physics 2000*, edited by A. Fokas, A. Grigoryan, T. Kibble, and B. Zegarlinsky (Imperial College, London, 2000), p. 128.
 - [20] S. Lepri, R. Livi, and A. Politi, *Phys. Rep.* **377**, 1 (2003).
 - [21] A. Dhar, *Adv. Phys.* **57**, 457 (2008).
 - [22] E. B. Davies, *J. Stat. Phys.* **18**, 161 (1978).
 - [23] C. Kipnis, C. Marchioro, and E. Presutti, *J. Stat. Phys.* **27**, 65 (1982).
 - [24] C. Giardinà, J. Kurchan, and F. Redig, *J. Math. Phys.* **48**, 033301 (2007).
 - [25] G. Basile, C. Bernardin, and S. Olla, *Phys. Rev. Lett.* **96**, 204303 (2006).
 - [26] S. Lepri, C. Mejia-Monasterio, and A. Politi, *J. Phys. A: Math. Theor.* **42**, 025001 (2009).
 - [27] H. Bufferand, G. Ciraolo, P. Ghendrih, P. Tamain, F. Bagnoli, S. Lepri, and R. Livi, *J. Phys.: Conf. Ser.* **260**, 012005 (2010).
 - [28] N. H. R. Kubo and M. Toda, *Statistical Physics II: Nonequilibrium Statistical Mechanics* (Springer, New York, 1985).
 - [29] A. Kundu, A. Dhar, and O. Narayan, *J. Stat. Mech.: Theory Exp.* (2009) L03001.
 - [30] D. D. Joseph and L. Preziosi, *Rev. Mod. Phys.* **61**, 41 (1989).
 - [31] F. Piazza and S. Lepri, *Phys. Rev. B* **79**, 094306 (2009).
 - [32] O. V. Gendelman and A. V. Savin, *Phys. Rev. E* **81**, 020103 (2010).
 - [33] K. K. Lin and L. S. Young, *J. Stat. Phys.* **128**, 207 (2007).
 - [34] H. Bufferand, B. Bensiali, J. Bucalossi, G. Ciraolo, P. Genesio, Ph. Ghendrih, Y. Marandet, A. Paredes, F. Schwander, E. Serre, and P. Tamain, *J. Nucl. Mater.* (2013), doi: 10.1016/j.jnucmat.2013.01.090.